Int. J. Pharm. Investigation, 2025; 15(1):138-158.
https://www.jpionline.org

Original Article

QBD-Based Optimization and Formulation of Doxorubicin Bcl-2 SIRNA-Loaded Sphingosomes

Prashant Nayak[1], Rompicherla Narayana Charyulu[1,*], Alandur Veena Shetty[2]

[1]Department of Pharmaceutics, NITTE (Deemed to be University), NGSM Institute of Pharmaceutical Sciences, Deralakatte, Mangalore, Karnataka, INDIA.
[2]Department of Microbiology, KS Hegde Medical Academy, NITTE (Deemed to be University), Deralakatte, Mangalore, Karnataka, INDIA.

ABSTRACT

Background: By increasing drug stability and water solubility, cycle duration, rate of absorption into target cells or tissues, and reducing enzymatic degradation, Nano Drug Delivery Systems (NDDS) improve the safety and effectiveness of drugs. The Sphingosomes have better drug retention properties and are significantly more resilient to acid hydrolysis. siRNAs are mostly used to silence post-transcriptional gene expression in cancer treatment. Doxorubicin is a known anticancer drug for lung cancer. **Materials and Methods:** The study shows how to use a 3^2 complete factorial design to optimize a bcl2 SIRNA-doxorubicin-loaded sphiongosome for the treatment of lung cancer. The drug was aimed at reducing the toxicity of the drug and in the treatment of multiple drug-resistant tumors. Nano forms of Sphingosomes were prepared using the thin film hydration process, and optimization was carried out using 3^2 full factorial designs in conjunction with the desirability function. Ten formulations with various drugs: lipid and sphingomyelin: cholesterol ratios were created, and their entrapment effectiveness, PDI, and vesicle size were assessed. An analysis of variance was used to determine the model's statistical validity (ANOVA). Contoured plots and response surface graphs were used to analyze the influence of variables on responses. Entrapment effectiveness and vesicle size data were discovered to be extremely similar to the predicted values. **Results:** The formulation was found to be spherical with an average diameter of 263.4 nm, PDI of 0.198, entrapment efficiency of 69.2, and -33.4 mV zeta potential. Results from TEM demonstrated the 200 nm particle size. DSC studies proved thermal peaks were in range. FTIR results of the physical mixture and the formulation were in the range and there was no physical incompatibility, According to serum stability, the formulation was resistant to nuclease digestion for 12 hr. The sterility test proved the formulation was sterile. **Conclusion:** The outcomes show that the QbD technique in sphingosome creation can enhance the formulation process. The creation of the DOX siRNA sphingosome formulation can be optimized and rationalized with the use of cutting-edge design and development methodologies.

Keywords: Doxorubicin, Sphingosome, Serum stability, Sterility, Zeta potential.

Correspondence:
Dr. Rompicherla Narayana Charyulu
Department of Pharmaceutics, NITTE (Deemed to be University), NGSM Institute of Pharmaceutical Sciences, Deralakatte-575018, Mangalore, Karnataka, INDIA.
Email: narayana@nitte.edu.in

Received: 14-06-2024;
Revised: 14-06-2024;
Accepted: 28-08-2024.

INTRODUCTION

Nano-Drug Delivery Systems (NDDS) enhance therapeutic safety and effectiveness by improving drug stability and water solubility, prolonging cycle times, accelerating uptake into target cells or tissues, and reducing enzymatic degradation. NDDS, which consist of nanoparticles, have emerged as a key tool in pharmacy and contemporary biomedicine for enhancing drug delivery. These systems encompass materials with at least one dimension on the nanoscale (1-100 nm), and can be organic, inorganic, or composite in nature.[1-3]

Sphingosomes, a prominent lipid vesicle drug delivery system, features a membranous lipid bilayer enclosing an aqueous space for drug entrapment. Composed of natural or synthetic sphingolipids along with cholesterol, sphingosomes offer advantages such as enhanced stability to acid hydrolysis and improved retention properties compared to liposomes and noisesomes. Sphingosomes can be administered through various routes including parenteral, oral inhalation, and transdermal.[4-7]

Advantages of the Sphingosomes System[8]

- Active targeting through coupling with site-specific ligands.
- Enhanced passive targeting in tumor tissue.
- Increased therapeutic index and efficacy.
- Improved stability and reduced toxicity of encapsulated agents.

OPEN ACCESS

Manuscript TECHNOMEDIA

DOI: 10.5530/ijpi.20251766

Publishing Partner : Manuscript Technomedia. [www.mstechnomedia.com]

- Enhanced pharmacokinetic effects.
- Classification of Sphingosomes.

Sphingosomes are classified based on structural characteristics including the number of bilayers and vesicle diameter. They can be categorized as Small Unilamellar Vesicles (SUVs), Large Unilamellar Vesicles (LUVs), Multilamellar Vesicles (MLVs), Oligolamellar Vesicles (OLVs), and Multivesicular Vesicles (MVVs), each with specific size ranges and structural features.[9-11]

Sphingosomes Composition

Comprising sphingolipids (e.g., sphingomyelin) and cholesterol, sphingosomes exhibit an acidic intracellular pH ratio, providing benefits such as improved drug retention and resistance to acid hydrolysis. Sphingolipids, originally named by J.L.W. Thudichum in 1884, have hydrophobic bodies and polar heads, affecting the structure and composition of lipids in human skin.[12-14]

Small-interfering RNA and Gene Silencing

RNA interference (RNAi), involving gene silencing via small interfering RNAs (siRNAs), represents a significant advancement in biology. SiRNAs are utilized for post-transcriptional gene expression silencing, facilitating targeted therapy for various diseases including cancer. Synthetic siRNAs are designed to target specific genes responsible for disease states, offering a promising approach for therapeutic applications.[15-19]

Doxorubicin and Nano Carriers

Doxorubicin (DOX), an anthracycline antibiotic, exhibits potent anti-tumor activity but faces challenges such as multidrug resistance. Nano carriers, including sphingosomes, offer strategies to enhance the therapeutic efficacy of DOX and minimize its adverse effects, with potential applications in cancer treatment.[20-24]

Response Surface Methodology (RSM) and Design of Experiments (DoE) are utilized for formulation optimization, analyzing the multifactorial interactions between formulation variables and their effects on dependent variables. These statistical approaches aid in the development of optimized drug delivery systems, such as siRNA-Dox-loaded sphingosomes, with the aim of enhancing efficacy and reducing toxicity.[25-30]

MATERIALS AND METHODS

Materials

Doxorubicin (Yarrow Chemical, Mumbai), Cholesterol (HI media, Mumbai), Sphingomyelin (Sigma Aldrich, Bangalore), siRNA (Takara bio-India limited, Bangalore). DMEM and Fetal Bovine Serum (HiMedia, Mumbai).

Formulation of doxorubicin and sphingosomes by Design of experiments (DoE) approach

Different ratio of doxorubicin and lipid for the formulation was selected according to the literature study and optimization was planned by DOE software.[31-34]

Based on the initial studies done and literature, the factors which influenced the formation of sphingosomes formulation were recognized. The concentration of medication lipid ratio and the sonication time were the main factors found. Using Design Expert® software (Version 11), the effect of these factors on dependent variables including vesicle size, PDI, and drug entrapment efficiency was examined using the quadratic response surface design represented by the second order polynomial model. An organised investigation of the formulations is made possible by the statistical and mathematical techniques that make up the Response Surface Methodology (RSM). Utilising response surface methodology, the method enables optimisation of the numerical factors that can affect the response surface, allowing for the quantification of the relationship between the numerical parameters at various levels.[35]

In a three level factorial randomized quadratic design with 10 experimental trials, the independent components drug: lipid ratio (A-W:W) and sonication time (min) were each chosen at three different levels, low (-1), medium (0), and high (+1).[36] The quadratic equation that follows, which includes polynomial terms, coefficient effects, and interactions, can be used to describe the implied model.

$$Y=b0+b1X1+b2X2+b12X1X2+b11X12+b22X22+\ldots \quad \text{(Eq. 1)}$$

Where Y is the measured response tied to each component level combination, X1 and X2 are the coded levels of independent variables, b0 is an intercept, and b1 through b22 are regression coefficients calculated from the observed experimental values of Y. Table 1 contains the experimental setup and actual values for the independent variables, whereas Table 2 displays the results of runs at various concentrations and sonication times.

Statistical Analysis

Contour Plots

Using Minitab 17 (CA, USA), contour plots were created to examine the impact of several input variables, including hydration time, hydration volume, drug: lecithin ratio, and quality features. The experimental data from the testing dataset was used to create the contour plots.

Response Surface Plots

Using Minitab 17 (CA, USA), the response surface plots were created to examine the impact of various input factors on quality metrics. The experimental findings from the testing dataset were used to create the response surface plots.

Table 1: 3^2 factorials design for sphingosome formulations of doxorubicin HCl: coded levels and actual values for each factor.

Factors	Levels, actual (coded)		
	-1 (Low)	0 (Medium)	+1 (High)
Independent variables	1:110	1:215	1:320
A=Doxorubicin HCl: sphingosomes (W:W) B=Sonication time (min)			
Dependent variables			
R1=Particle Size (nm) (R1)R2=PDI R3=Entrapment efficiency (%) (R2)			

Table 2: Formulations given by the DOE software considering drug: polymer ratio and sonication time factors.

	Factor 1	Factor 2
Run	A: Drug: Lipid Ratio	B: Sonication time
		min
1	0	-1
2	0	1
3	1	0
4	1	-1
5	-1	1
6	-1	-1
7	0	0
8	1	1
9	-1	0
10	0	0

Preparation of doxorubicin sphingosomes

Using Buchi rotavapor R 200 the sphingosomes were prepared by thin film hydration procedure. Variable amounts of sphingolipid, cholesterol, and medication were dissolved in around 50 mL of chloroform to create the formulations.[37] After that, the solution was poured into a 500 mL round-bottom flask. To create a thin layer, chloroform was evaporated using a rotating evaporator at 63°C and a vacuum of 100 mmHg. Up until dry residue was created, evaporation was continued for roughly 15 min. By using this technique, the organic solvent is progressively removed, leaving a thin lipid layer on the flask's interior surface. The films were vacuum dried for an entire night in order to assure complete evaporation of the organic solvent. After that, the film was hydrated with various volumes (90, 105, and 120 mL) of phosphate buffer with a pH of 7.4.[38,39]

Size Reduction by Sonication

A Fisher Scientific sonic dismembrator (model F50) with a probe sonicator was utilized for this approach. 40% was chosen as the percentage amplitude for the power applied to the solution. At room temperature, a probe sonicator was used to sonicate the sphingosomal solution for various durations-10 min, 15 min, and 20 min-at a depth of 19 mm from the base of the vessel.

Optimized Formulation of (SD)

From the above data obtained by Design of Experiments after conducting 10 runs the formulation was prepared and named as (SD). Software predicted values where drug lipid ratio value was zero it means dox drug was taken 0.01 g with 0.02 g of sphingomyelin plus 0.006 g of cholesterol. Data predicted for sonication time is 15 min sonication time.

The final formulation was prepared by taking the above ratio of the drug and will be sonicated for 15 min.

Evaluation of Optimized Formulation

Particle size, Polydispersity Index (PDI) and zeta potential

Using the Zetasizer Nanoseries from Malvern Instruments in Malvern, UK, and dynamic light scattering, the mean particle size, PDI, and zeta potential of nanoparticles were calculated. The data for size, PDI, and zeta potential were recorded after the samples were placed in a "folded capillary cell".[40]

Entrapment Efficiency

The amount of free drug in the supernatant was quantified spectrophotometrically at 483 nm after centrifuging the known quantity of nanoparticulate dispersion at 10000 RPM for 15 min

using a REMI centrifuge to determine entrapment efficiency. The equation was used to calculate the entrapment efficiency.[41]

Entrapment efficiency=(Amount of entrapped drug)/(Amount of total drug)x100(1.1)

Transmission Electron Microscopy (TEM)

The formulation was diluted with deionised water in the ratio of 1:20 and sonicated for 3 min then analyzed. CLCAE and CLAA drop inserted on a carbon-coated copper grid, which forms a liquid film. The film was negatively stained by adding a drop of ammonium molybdate (2% w/w) in 2% w/v ammonium acetate buffer (pH 6.8), on the grid. Filter paper is used to remove excess stain. The dried, stained film was examined under a transverse electron microscope.[42]

Differential Scanning Calorimetry (DSC) Utilising a DSC1 Mettler Toledo apparatus (Mettler Toledo, Greifensee, Switzerland), differential scanning calorimetry was carried out. The sample was heated from 250°C to 200°C with a scan rate of 100°C/min while it was contained in an aluminium pan and subjected to nitrogen flow (50 mL/min). Each sample underwent a triple analysis. The STARe programme 14.00 was used to analyse DSC curves.[43]

Fourier Transform Infrared Spectroscopic (FTIR) studies

Formulation SD was analysed by FTIR by Attenuated Total Reflectance method (ATR) in the wave number range of 400-4000 cm-1 By Bruker tensor FTIR, Physical mixture and formulation will be compared.[44]

Assay for serum stability test

siRNA-loaded sphingosomal nanoparticles used in the serum stability test were incubated at 37°C with an equivalent amount of DMEM supplemented with a 10% final dose of FBS. 30 µl of the mixture were taken at each predetermined time interval (0.5, 1, 2, 4, 8, 24, 48, and 72 hr) and kept at -20°C until gel electrophoresis was carried out. Samples were heated at 80°C in a bath incubator for 5 min to stop serum activity, and then 5 L of heparin (1000 U/mL) was added to remove the siRNA from the formulation. After then, a 1.5% agarose gel containing ethidium bromide was used to examine the siRNA's integrity.[1] Tris Acetate EDTA (TAE) buffer was electrophoresed for 1 hr at a constant voltage of 50 V. At a wavelength of 365 nm, siRNA bands were seen using a UV transilluminator.[45,46]

Sterility Testing

To assure the sterility of the finished product, sterility tests were conducted. Direct inoculation was chosen above other testing methods since it is administered via parenteral route. According to this procedure, the required amount of sample was aseptically removed from the containers and transferred to separate fluid thioglycollate (20 mL) and soybean-casein digest (20 mL) mediums. Incubation of the nanoparticle mixture with the medium took place for a minimum of 14 days at 36°C and RH 50% for fluid thioglycolate medium and 26°C and RH 50% for soybean-casein digest media. Any type of microbial development in the media was noticed.[47]

Bacteria taken for the test was *S. aureus* ATCC number 23235.

The fungus taken for the test was *Candida albicans* ATCC number 10231.

By selecting *S. aureus* ATCC 23235 and *C. albicans* ATCC 10231, the sterility testing process can comprehensively assess the effectiveness of sterilization methods against both bacterial and fungal contaminants, ensuring the safety and quality of sterile products.

RESULTS

Statistical analysis by experimental design

The vesicle size of all the formulations was ranging from 186 to 338, PDI was 0.153-0.277, and percentage entrapment effectiveness was found to be in scope of 63.7 to 82.8 as shown in Table 3. ANOVA for Linear model, Response 1: Vesicle Size.

The model is suggested to be significant by the model's F-value of 10.43. An F-value this large might be caused by noise only 0.80% of the time. Model terms are considered significant when the *p*-value is less than 0.0500. B is a crucial model term in this instance. Model terms are not significant if the value is higher than 0.1000. Model reduction may enhance your model if it has a lot of unnecessary terms (except those needed to maintain hierarchy).

According to Table 4, there is a 5.59% probability that the big Lack of Fit F-value of 187.35 could be the result of noise. The model should fit; a lack of fit is undesirable. It is concerning that this chance is so low (10%).

As can be seen in Table 5, the Predicted R2 of 0.4149 is not as near to the Adjusted R2 of 0.6769 as one might often anticipate. This can be a sign of a significant block effect or a potential issue with your model and/or data. Model reduction, response transformation, outliers, etc. are things to think about. Confirmation runs should be used to test all empirical models.

The equations generated for the response particle size based upon the quadratic model in terms of coded and actual factors are written below.

Vesicle Size=+250.71+5.53A*-44.78B*

A*=drug:lipid ratio(w:w).

B*=sonication time (min).

Contour and 3D surface plots

Figures 1 and 2 displays the contour plot and the 3D surface plot for the response vesicle size. According to the plots, the vesicle size decreased as the concentration of drug-lipid increased up to a certain point, but as the concentration of drug-lipid ratio increased further, the vesicle size increased and the effect of drug-lipid ratio was found to be less significant. The vesicle size was observed to steadily decrease as the sonication time was increased, making the influence of sonication time on vesicle size more substantial.

The model is implied to be significant by the Model F-value of 6.48. As indicated in Table 6, there is only a 4.72% possibility that noise could cause an F-value this significant.

Model terms are considered significant when the *p*-value is less than 0.0500. A2 is a crucial model term in this instance. Model terms are not significant if the value is higher than 0.1000. Model reduction may enhance your model if it has a lot of unnecessary terms (except those needed to maintain hierarchy).

The F-value for the lack of fit, 3.14 indicates that the lack of fit is not significant in comparison to the pure error. A "Lack of Fit F-value" this large could be caused by noise with a 38.81% probability.

Non-significant lack of fit is good we want the model to fit.

As one could typically anticipate, the Predicted R2 of 0.1188 is more than 0.2 away from the Adjusted R2 of 0.7527. This can be a sign of a significant block effect or a potential issue with your model and/or data. Model reduction, response transformation,

Table 3: 3^2 factorial quadriatic design experimental batches for entrapment efficiency, vesicle size and PDI.

	Factor 1	Factor 2	Response 1	Response 2	Response 3
Run	A: Drug: Lipid Ratio	B: Sonication time	Vesicle Size	PDI	EE
		min	nm	-	%
1	0	-1	338±0.86	0.148±0.36	72.5±0.82
2	0	1	186±0.37	0.182±0.64	70.7±0.27
3	1	0	241.9±0.53	0.206±0.92	82.8±0.82
4	1	-1	300.5±0.15	0.228±0.48	77.8±0.49
5	-1	1	229.2± 0.34	0.29±0.39	68.3±0.28
6	-1	-1	264.2±0.81	0.277±0.61	63.7±0.83
7	0	0	248.3±0.62	0.174±0.37	76.6±0.67
8	1	1	218.8±0.84	0.232±0.67	80.2±0.73
9	-1	0	234.6±0.57	0.214±0.29	65.4±0.64
10	0	0	245.6±0.63	0.153±0.37	74.8±0.37

Table 4: ANOVA table for vesicle size.

Source	Sum of Squares	d_f	Mean Square	F-value	*p*-value	Significance
Model	12216.99	2	6108.49	10.43	0.0080	Significant
A-Drug: Lipid Ratio	183.71	1	183.71	0.3136	0.5930	
B-Sonication time	12033.28	1	12033.28	20.54	0.0027	
Residual	4100.96	7	585.85			
Lack of Fit	4097.32	6	682.89	187.35	0.0559	Not significant
Pure Error	3.65	1	3.65			
Cor Total	16317.95	9				

Table 5: Fit Statistics of vesicle size.

Std. Dev.	24.20	R^2	0.7487
Mean	250.71	Adjusted R^2	0.6769
C.V. %	9.65	Predicted R^2	0.4149
		Adeq Precision	7.5908

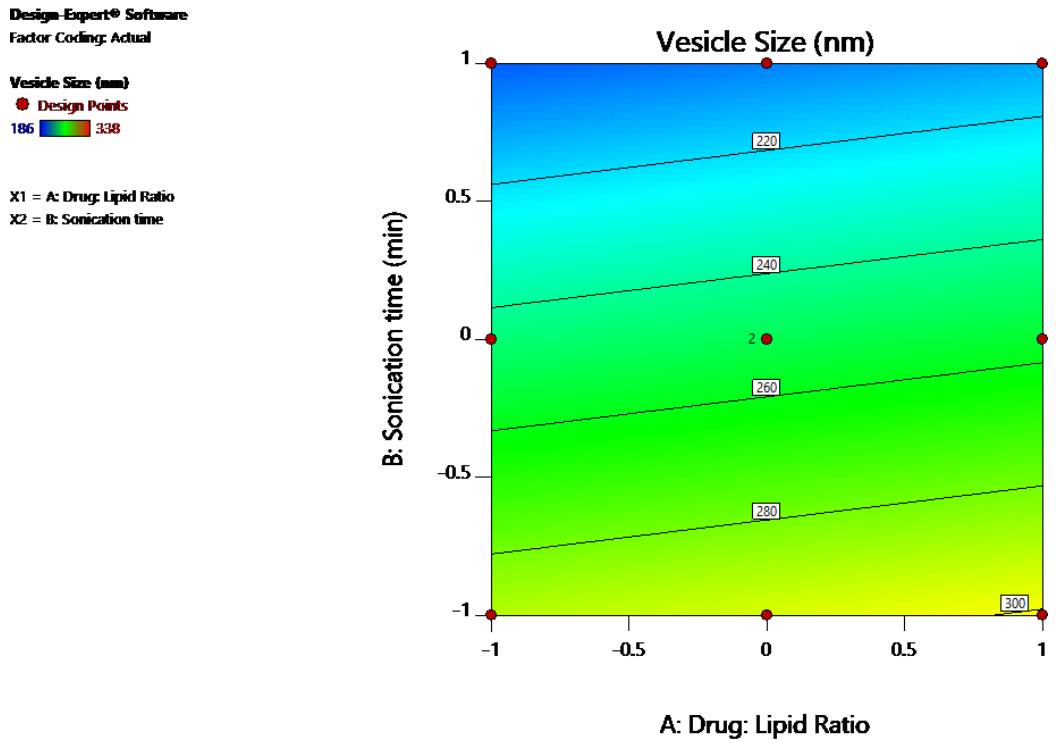

Figure 1: 3D surface plot of vescile size (nm) against drug: lipid and sonication time (min).

Table 6: ANOVA for Quadratic model of PDI.

Source	Sum of Squares	d_f	Mean Square	F-value	*p*-value	Significance
Model	0.0186	5	0.0037	6.48	0.0472	Significant
A-Drug: Lipid Ratio	0.0022	1	0.0022	3.84	0.1217	
B-Sonication time	0.0004	1	0.0004	0.7548	0.4340	
AB	0.0000	1	0.0000	0.0353	0.8602	
A^2	0.0122	1	0.0122	21.27	0.0099	
B^2	0.0017	1	0.0017	3.04	0.1562	
Residual	0.0023	4	0.0006			
Lack of Fit	0.0021	3	0.0007	3.14	0.3881	Not significant
Pure Error	0.0002	1	0.0002			
Cor Total	0.0209	9				

outliers, etc. are things to think about. Confirmation runs should be used to test all empirical models.

The F value and P value for the quadratic model of response entrapment PDI were found to be 30.01 and 0.0029 and the model was found to be significant. The ANOVA response for PDI was shown in Table 7.

The equations generated for the response PDI based upon the quadratic model in terms of coded Factors are written below.

$$PDI=+0.1506-0.0192A^*+0.0085B^*-0.0022AB^*+0.0724A^{*2}+0.0274B^{*2}$$

A*=drug:lipid ratio (w:w).

B*=sonication time (min).

Contour and 3D surface plots

Figures 3 and 4 displays the contour plot and the 3D surface plot for the response PDI. PDI reduced when the concentration of drug-lipid was increased up to a certain point, but as the concentration of drug-lipid ratio was increased further, PDI increased and the effect of drug-lipid ratio was shown to be less significant. Since the PDI was observed to steadily decrease as the sonication duration was increased, the influence of sonication time on PDI was shown to be more significant. ANOVA for Linear model, Response 3: EE.

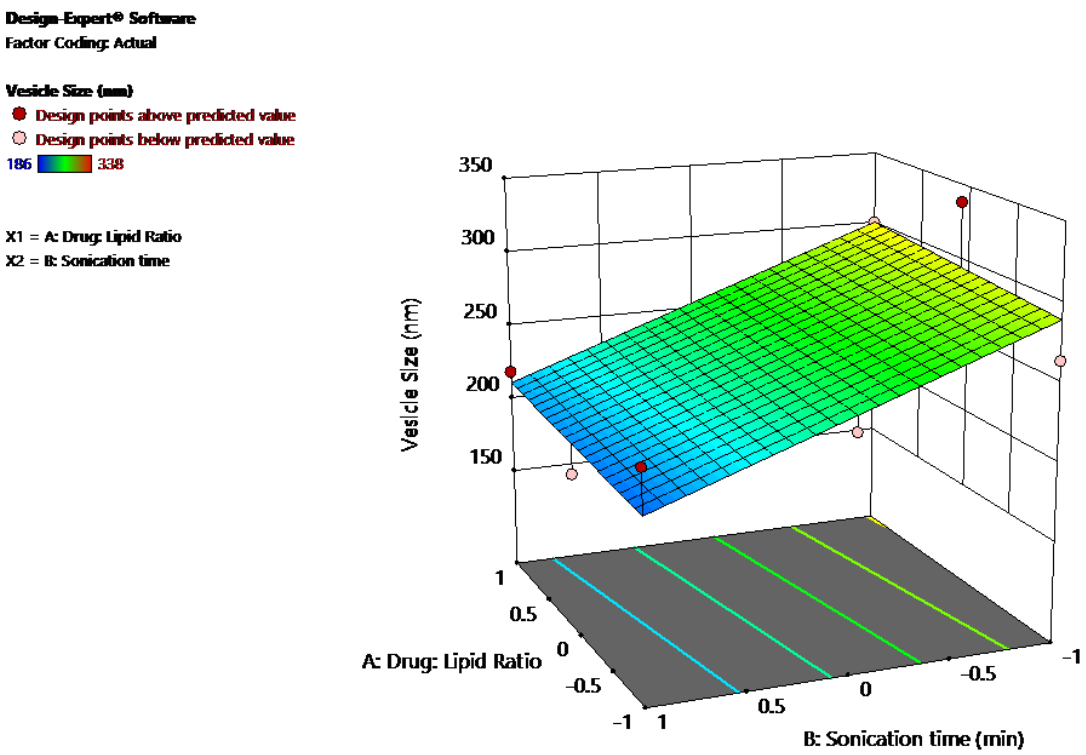

Figure 2: Contour plot of particle size (nm) against drug: lipid and sonication time (min).

Table 7: Fit Statistics of PDI.

Std. Dev.	0.0240	R^2	0.8901
Mean	0.2104	Adjusted R^2	0.7527
C.V. %	11.39	Predicted R^2	0.1188
		Adeq Precision	6.9831

Table 8: ANOVA for Linear model of EE.

Source	Sum of Squares	df	Mean Square	F-value	*p*-value	Significance
Model	318.43	2	159.22	28.02	0.0005	Significant
A-Drug: Lipid Ratio	313.93	1	313.93	55.24	0.0001	
B-Sonication time	4.51	1	4.51	0.7930	0.4028	
Residual	39.78	7	5.68			
Lack of Fit	38.16	6	6.36	3.93	0.3682	Not significant
Pure Error	1.62	1	1.62			
Cor Total	358.22	9				

Table 9: Fit Statistics of EE.

Std. Dev.	2.38	R^2	0.8889
Mean	73.28	Adjusted R^2	0.8572
C.V. %	3.25	Predicted R^2	0.7855
		Adeq Precision	12.4067

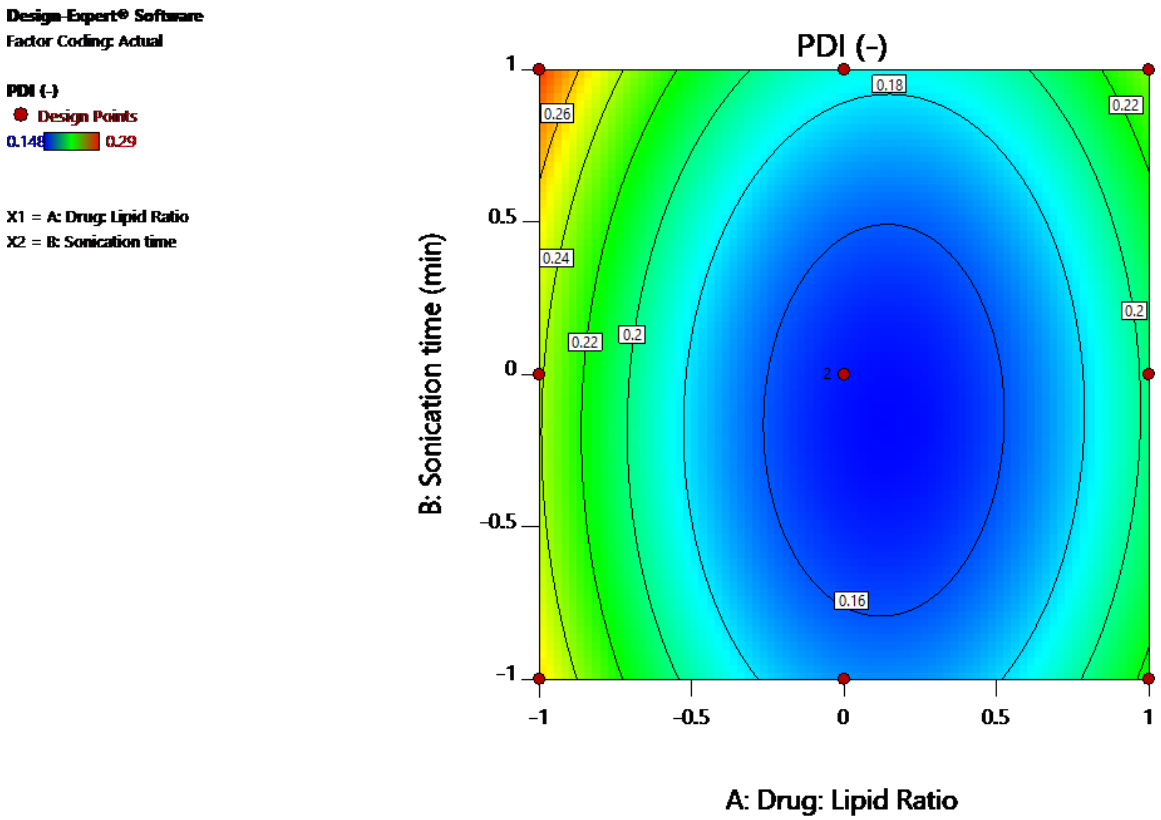

Figure 3: Contour plot of PDI against drug: lipid and sonication time (min).

The model is apparently important given its Model F-value of 28.02. An F-value this large might happen as a result of noise only 0.05% of the time.

Model terms are considered significant when the *p*-value is less than 0.0500. A is a significant model term in this instance. Model terms are not significant if the value is higher than 0.1000. Model reduction may enhance your model if it has a lot of unnecessary terms (except those needed to maintain hierarchy).

The lack of fit is implied to be insignificant in comparison to the pure mistake by the lack of fit F-value of 3.93. A "Lack of Fit F-value" this large could be caused by noise with a 36.82% probability. We want the model to fit, thus a non-significant lack of fit is ideal as shown in Table 8.

As shown in Table 9 the Predicted R^2 of 0.7855 and the Adjusted R^2 of 0.8572 are reasonably in agreement, therefore the difference is less than 0.2.

The ratio of signal to noise is measured by Adeq Precision. A ratio of at least 4 is preferred. Your ratio of 12.407 shows a strong enough signal. To move around the design space, utilise this model. Final Equation in Terms of Coded Factors.

EE=+73.28+7.23A*+0.8667B*

A*=drug:lipid ratio(w:w).

B*=sonication time (min).

Contour and 3D surface plots

Figures 5 and 6 displays the contour plot and the 3D surface plot for the response EE. According to the plots, EE reduced when drug-lipid concentration was raised to a certain point and then increased as drug-lipid concentration was raised further, with the influence of the drug-lipid ratio being determined to be less significant. Since the EE was observed to steadily decrease as the sonication duration rose, the effect of sonication time on EE was determined to be more important.

Point Prediction

Two-sided; Confidence=95%; Population=99%; Point Prediction.

Response prediction

For optimized formulation the predicted mean for particle size and drug content was analyzed by comparing with the 95% confidence interval of mean. It was found that the predicted mean was within the 95% confidence interval which is shown in Table 10.

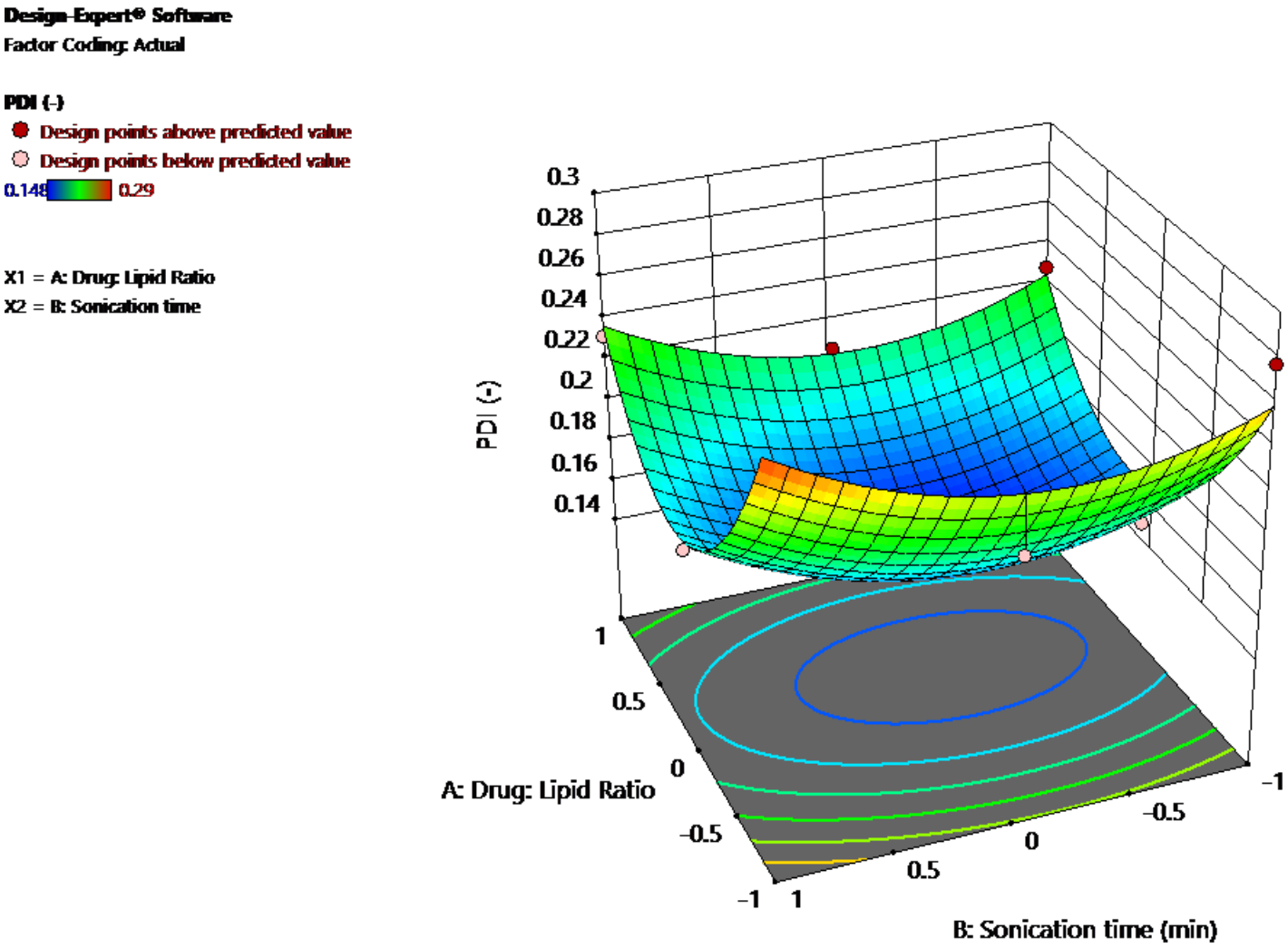

Figure 4: 3D surface plot of PDI against drug: lipid and sonication time (min).

Table 10: Point of prediction: Generated predicted responses for selected solution.

Response	Predicted Mean	Predicted Median	Observed	Std Dev	SE Mean	95% CI low for Mean	95% CI high for Mean	95% TI low for 99% Pop	95% TI high for 99% Pop
Vesicle Size	250.71	250.71	230.71	24.2044	7.65409	232.611	268.809	124.163	377.257
PDI	0.150571	0.150571	0.195	0.0239654	0.0143221	0.110807	0.190336	-0.0264087	0.327552
EE	73.28	73.28	75.6	2.38395	0.753873	71.4974	75.0626	60.816	85.744

Table 11: Confirmation table Two sided for 95% confidence.

Response	Predicted Mean	Predicted Median	Observed	Std Dev	n	SE Pred	95% PI low	Data Mean	95% PI high
Vesicle Size	250.71	250.71	230.71	24.2044	2	18.7486	206.377	268.35	295.043
PDI	0.150571	0.150571	0.195	0.0239654	2	0.0221877	0.0889685	0.186	0.212174
EE	73.28	73.28	75.86	2.38395	2	1.8466	68.9135	70.65	77.6465

Confirmation

The selected formulation showed standard deviation value of 24.2044 vesicle size, 0.0239654 PDI, and 2.38395 EE as shown in Table 11.

Confirmation

Two-sided; Confidence=95%.

From Table 12 the drug lipid ratio is 0 means 1 and the sonication time is found to be 15 min.

From Table 13 the predicted values of vesicle size is from 263.4 to 273.3 and PDI was found as 0.198 and 0.174 the EE was 69.2-72.1 respectively.

From Table 14 formulation selected was called SD which contains a drug: lipid ratio of 0and the sonication time was 15 min. The dependent variables of predicted values in the case of vesicle size showed a 5.23% error, PDI when compared showed a % error of 4.27, and percentage drug entrapment was found to be a 3.52% error.

Table 12: Confirmation of Location of formulation.

Drug: Lipid Ratio	Sonication time
0	0

Table 13: Formulation range predicted by DOE.

Vesicle Size	PDI	EE
263.4	0.198	69.2
273.3	0.174	72.1

Results of Optimized Formulation SD

The particle size of the formulation from the Table 15 was found to be 230.7 nm, The PDI of the formulation was found to be 0.195, Result quality of the formulation was found to be good.

Result quality: Good.

From the Table 16 and Figure 7 the zeta potential was -33.4 mV.

Entrapment Efficiency

Percentage Entrapment efficiency of the formulation SD was found to be 75.86%.

The free drug/un trapped drug which was collected after centrifugation and UV absorbance was taken which was substituted from the equation of y=0.0118x-0.003 which was obtained from calibration curve of dox. The concentration found was concentration of the free drug which was substituted in equation and the final value of the EE of SD formulation was found to be 75.86%.

Table 14: Solution and the % error between observed and predicted values.

	Independent variables	Predicted	Formulation response	
Factors	A: Drug: lipid Ratio	0	Dox drug 0.01 g with 0.02 g of sphingomyelin plus 0.006 g of cholesterol and sonication time 15 min.	
	B: Sonication Time	0		
	Dependent variables	Predicted	Actual	% error
Response	Vesicle size (nm)	243. 45	230.71	5.23
	PDI	0.187	0.195	4.27
	Drug Entrapment (%)	73.28	75.86	3.52

Table 15: Particle Size, Polydispersity Index (PDI).

Parameter	Value	Peak	Size in nm	%Intensity:	Standard Deviation
Z-Average (d.nm):	230.7	Peak1:	242.2	100.0	78.70
PdI:	0.195	Peak2:	0.000	0.0	0.000
Intercept:	0.938	Peak3:	0.000	0.0	0.000
Result quality	Good				

Table 16: Results of zeta potential.

Parameter	Value	Peak	Mean (mV)	Area (%)	Width (mV)
Zeta Potential (mV):	-33.4	Peak 1:	-31.9	93.0	8.40
Zeta Deviation (mV):	10.2	Peak 2:	-57.1	7.0	4.24
Conductivity (mS/cm):	0.0219	Peak 3:	0.00	0.0	0.00

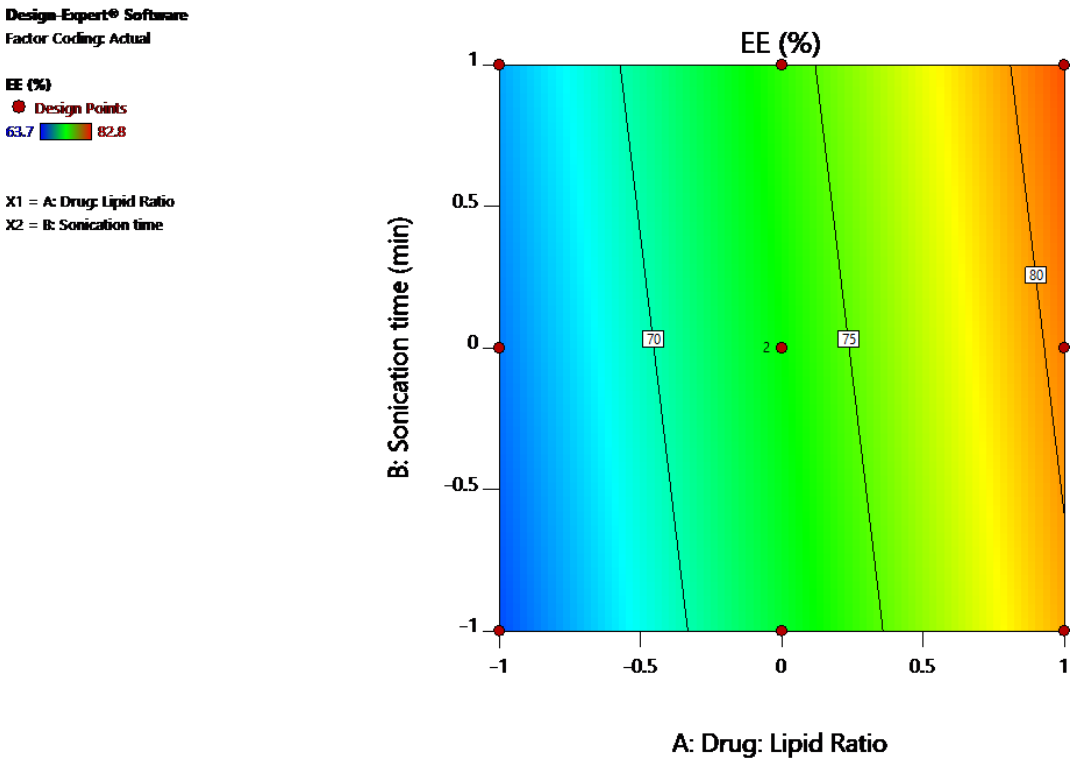

Figure 5: Contour plot of EE against drug: lipid and sonication time (min).

Transmission Electron Microscopy (TEM)

The TEM image in Figure 8 illustrates the Transmission Electron Microscopy (TEM) image, showing that the particles in the formulation demonstrated variability in size and were mainly spherical in shape and had smooth surfaced texture. The particle size analysis of the SD formulation indicates that the particles ranged in size from approximately 145-205 nm.

Differential Scanning Calorimetry (DSC)

DSC was done for the pure drug and formulation thermal doxorubicin was 232.43 and the formulation was found to have 215.30 thermal peak which proves the thermal peaks are in range. DSC exhibited single endothermic peak at 158.34 in pure drug and in formulation it was found to be 161.95 for cholesterol. In case of sphingomyelin a peak of 178.25 of pure drug and formulation was found to be 183.88. These thermal peaks were in the respective range as shown in Figures 9-12 and Table 17.

FTIR studies

The functional groups of the individual compounds and the physical mixture were recorded and the formulation functional groups were compared it was found the peaks obtained in the physical mixture and the formulation were in the range and there was no physical incompatibility in the compoundsC=O stretching, O-H stretching NH_2 stretching and -O- stretching peaks are shown in Figures 13-17 and Table 18.Serum stability studiesVisual analysis of band intensities revealed that naked siRNA had been intact for up to 1 hr. After that, there was a partial degeneration, and at 6 hr, there was a total degradation. For up to 4 hr, siRNA put in the formulation was shown to be intact. At 12 hr, there was some partial degradation; at 48 hr, there was total degradation of the siRNA. Nuclease digestion was prevented by the formulation (Figure 18 A and 18 B).

On visual examination of the intensities of bands, naked siRNA was found to be intact for up to 1 hr. Thereafter, partial degradation took place and at 6 hr, complete degradation was at 48 hours.

Sterility test

Formulations were incubated for 14 days at 30° to 35°C and RH (Relative humidity) of 50% in the case of fluid thioglycolate medium and at 20° to 25°C in the case of soybean-casein digest medium with RH pf 50%. As shown in Table 19 and Figure 19A and 19B, we detected no indication of microbial growth. The formula passes the sterility inspection.

DISCUSSION

Experimental Design and Statistical Analysis

The experimental design employed a 3^2 factorial quadratic design to assess the influence of drug-lipid ratio and sonication time on key parameters-vesicle size, Polydispersity Index (PDI), and Entrapment Efficiency (EE)-of the SD formulation.

Analysis of Vesicle Size

ANOVA results for vesicle size revealed a significant model (F-value=10.43, p=0.0080), indicating that both drug-lipid ratio

and sonication time significantly influenced vesicle size. The quadratic model equation predicted that vesicle size decreased with increasing sonication time but showed an initial decrease followed by an increase with drug-lipid ratio beyond a certain point. This behavior was corroborated by contour and 3D surface plots, highlighting the interactive effects of the factors.

Analysis of Polydispersity Index (PDI)

Similarly, the quadratic model for PDI showed significance (F-value=6.48, p=0.0472), with drug-lipid ratio (A) demonstrating a significant quadratic effect. The plots indicated that PDI decreased initially with an increase in drug-lipid ratio and sonication time, but further increases in drug-lipid ratio led to higher PDI values. Sonication time exhibited a less significant influence on PDI.

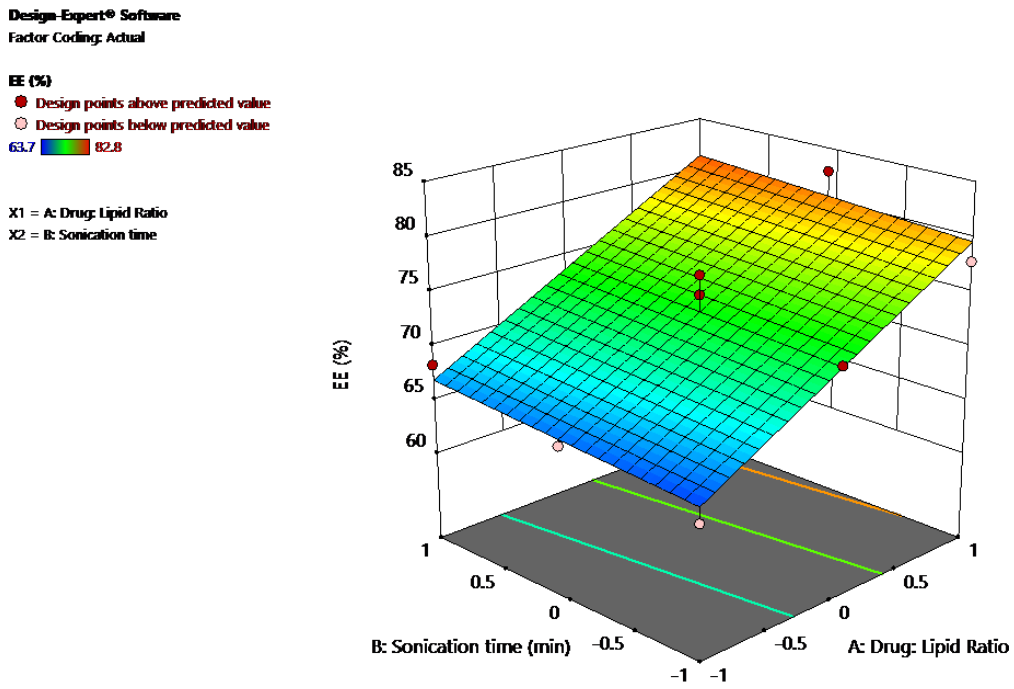

Figure 6: 3D surface plot EE against drug: lipid and sonication time (min).

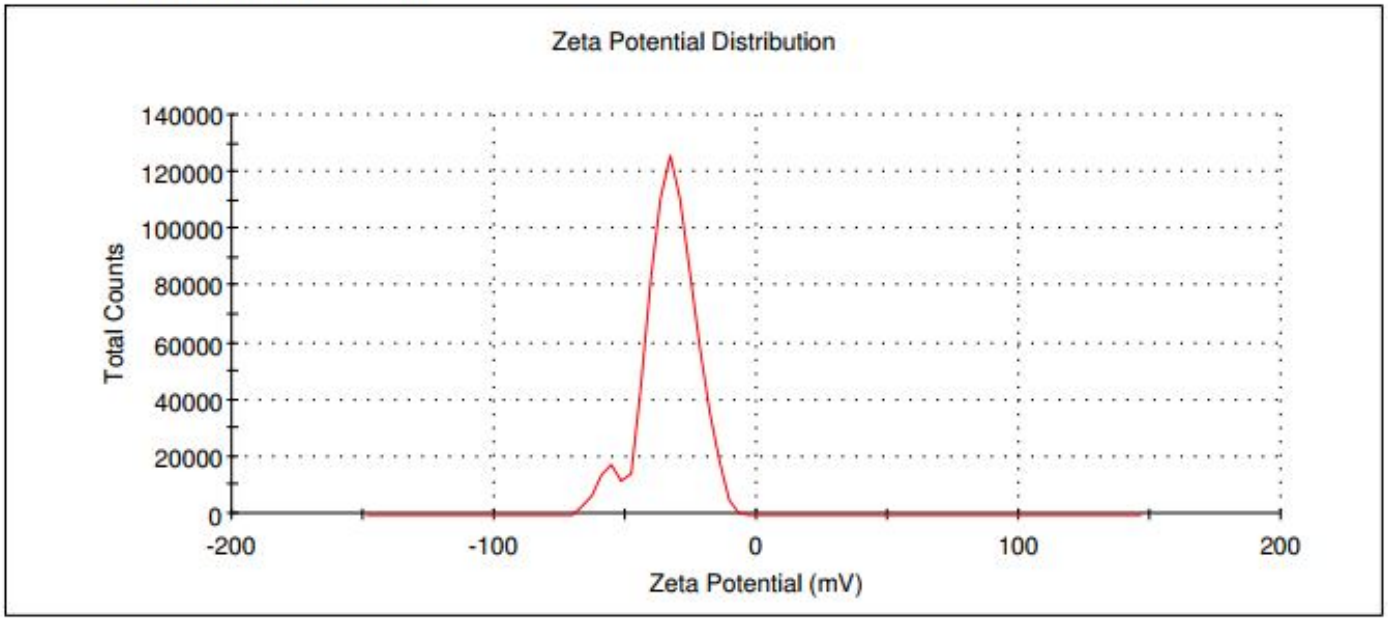

Figure 7: Zeta potential of the formulation SD.

Analysis of Entrapment Efficiency (EE)

The linear model for EE yielded a highly significant result (F-value=28.02, p=0.0005), where drug-lipid ratio (A) had a substantial positive effect. Sonication time (B), however, showed a non-significant influence on EE. The predicted and observed EE values were well within the 95% confidence interval, indicating the reliability of the model predictions.

Confirmation and Error Analysis

Confirmation runs validated the predicted values of vesicle size, PDI, and EE, showing minimal percent errors between predicted and observed values (5.23%, 4.27%, and 3.52% respectively). This affirmed the robustness of the selected formulation (SD) with a drug-lipid ratio of 0 and a sonication time of 15 min. The experimental design and statistical analysis provided valuable insights into optimizing the SD formulation for vesicle size, PDI, and EE. The quadratic models effectively captured the complex interactions between formulation parameters, guiding towards an optimized formulation with desirable characteristics for effective drug delivery. Future studies could further refine these models and explore additional factors to enhance formulation efficacy and consistency.

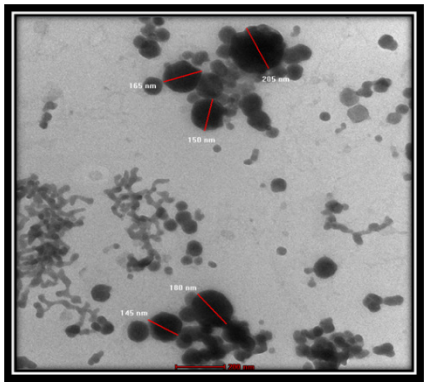

Figure 8: TEM image of the formulation SD.

Particle Size, PDI, and Zeta Potential

The SD formulation was characterized by analyzing particle size, polydispersity index (PDI), and zeta potential, crucial factors influencing formulation stability and efficacy.

Particle Size and PDI

The formulation exhibited a particle size of 230.7 nm (Table 15), ideal for drug delivery systems, facilitating effective encapsulation and potential cellular uptake. A low PDI of 0.195 indicated uniform particle size distribution, essential for consistent drug release and therapeutic effectiveness.

Zeta Potential

The formulation demonstrated a zeta potential of -33.4 mV (Table 16 and Figure 7), indicating good stability due to repulsive forces between particles. This property reduces aggregation, ensuring dispersion stability and contributing to the formulation's performance under physiological conditions.

Result Quality

Both particle size and zeta potential analyses indicated a "Good" result quality (Tables 15 and 16), underscoring the formulation's robustness and suitability for therapeutic use. These attributes collectively enhance its potential for efficient and safe drug delivery to targeted sites. SD formulation showcases favorable characteristics in particle size, PDI, and zeta potential, highlighting its promising application in drug delivery. These findings support its advancement and potential adoption in clinical settings, where reliability, uniformity, and effective drug release are critical.

Table 17: DSC thermal peaks of compounds and formulation SD.

Sl. No.	Sample	Thermal peaks of pure drug (C)	Formulation thermal peak (C)
1	Doxorubicin	232.43	215.30±01.03
2	Cholesterol	158.34	161.95±0.83
3	Sphingomyelin	178.25	183.88±1.37

Table 18: Interpretations of FTIR Spectra for pure drug.

Sl. No.	Functional Groups	Assessment Peak of dox	Assessment Peak of sphingolipid	Assessment peak of cholesterol	Assessment peak of physical mixture	Assessment peak of formulation SD
1	C=O Stretching	1729	1736	-----	1736	1623
2	O-H Stretching	3633	3797	3615	3706	3739
3	NH_2 Stretching	3519	-----	-----	3322	3374
4	-O- Stretching	1199	1228	-----	1231	1205

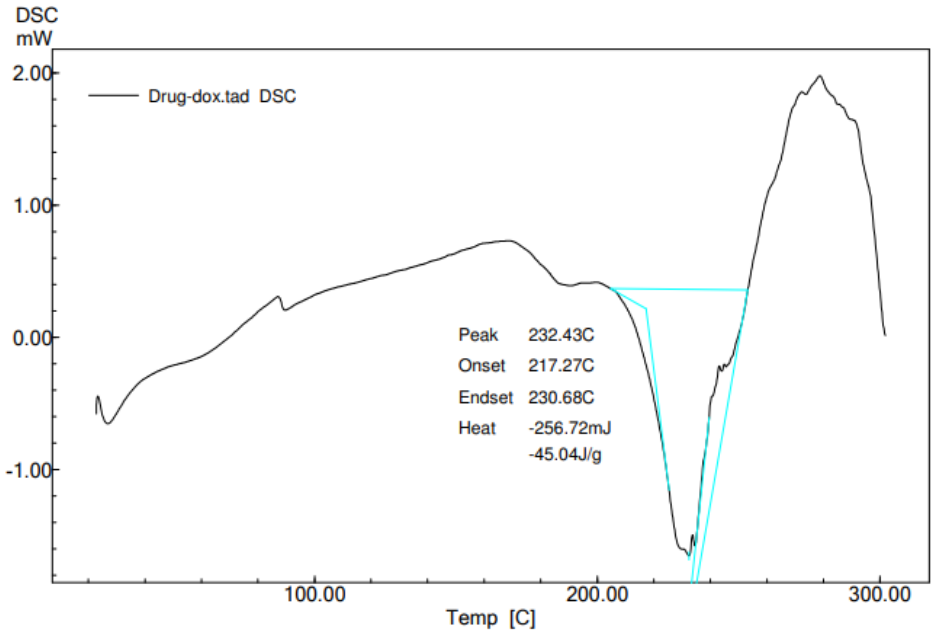

Figure 9: DSC thermal peaks of Doxorubicin.

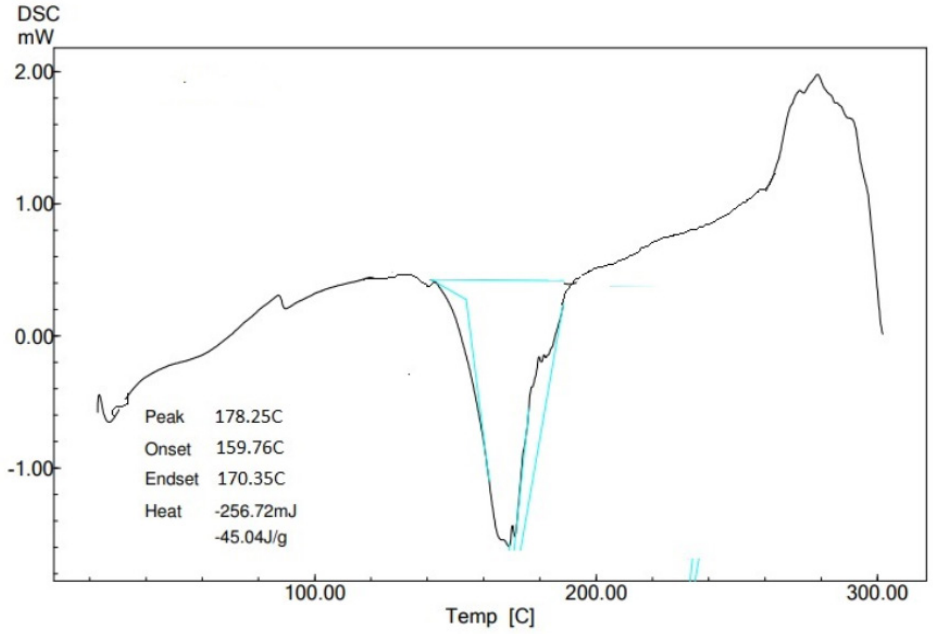

Figure 10: DSC thermal peaks of sphingomyelin.

Entrapment Efficiency

The Entrapped Efficiency (EE) of the SD formulation was determined to be 75.86%. This measure indicates the proportion of the drug that successfully remained encapsulated within the formulation after preparation, crucial for assessing its efficacy and dosage consistency.

To calculate EE, free drug concentrations were measured using UV absorbance after centrifugation and correlated with a calibration curve (y=0.0118x - 0.003). This method provided a precise determination of the amount of free drug, allowing for accurate substitution into the EE calculation equation.

Achieving an EE of 75.86% signifies efficient encapsulation, ensuring a significant portion of the drug remains protected within the formulation until delivery. This high EE is advantageous for therapeutic applications, as it maximizes drug stability, enhances

controlled release characteristics, and potentially reduces side effects by minimizing systemic exposure to free drug.

The TEM image in Figure 8 shows particles in the formulation ranging from 145 to 205 nm, predominantly spherical with a smooth surface texture.

This size range is ideal for drug delivery, suggesting effective encapsulation and enhanced cellular uptake. The spherical shape and smooth texture improve interaction with biological membranes, enhancing stability and efficacy. Overall, TEM analysis confirms the uniform and suitable morphology of the particles, supporting their potential effectiveness in drug delivery.

Differential Scanning Calorimetry (DSC) was performed to assess the thermal properties of the pure drug and the formulation. The thermal peaks of the pure drug and the formulation, as detailed in Table 17, demonstrate the stability and compatibility of the components.

Doxorubicin: The pure drug exhibited a thermal peak at 232.43°C, while the formulation showed a peak at 215.30°C. This shift indicates some interaction within the formulation but remains within an acceptable range.

Cholesterol: The DSC analysis showed a single endothermic peak at 158.34°C for the pure drug, and a peak at 161.95°C in

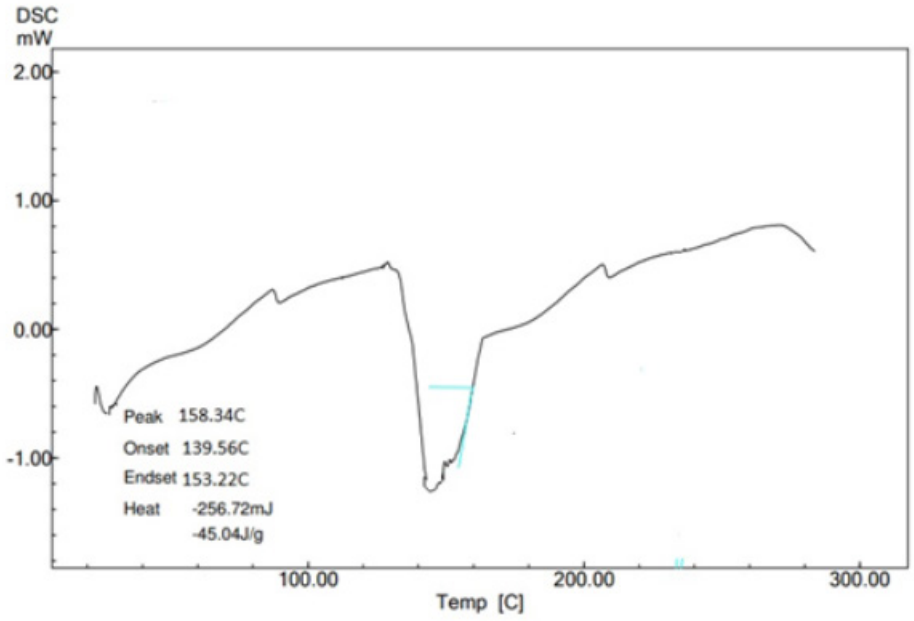

Figure 11: DSC thermal peaks of cholesterol.

Table 19: Results of Sterility test of formulation SD.

Test	Test	Days													
		1	2	3	4	5	6	7	8	9	10	11	12	13	14
Fluid thioglycollate medium	Sterility of medium	-	-	-	-	-	-	-	-	-	-	-	-	-	-
	Growth promotion test	+	+	+	+	+	+	+	+	+	+	+	+	+	+
	Sterility test of the formulation	-	-	-	-	-	-	-	-	-	-	-	-	-	-
Soyabean casein digest medium	Sterility of medium	-	-	-	-	-	-	-	-	-	-	-	-	-	-
	Growth promotion test	+	+	+	+	+	+	+	+	+	+	+	+	+	+
	Sterility test of the formulation	-	-	-	-	-	-	-	-	-	-	-	-	-	-

Indicates no growth+indicates growth.

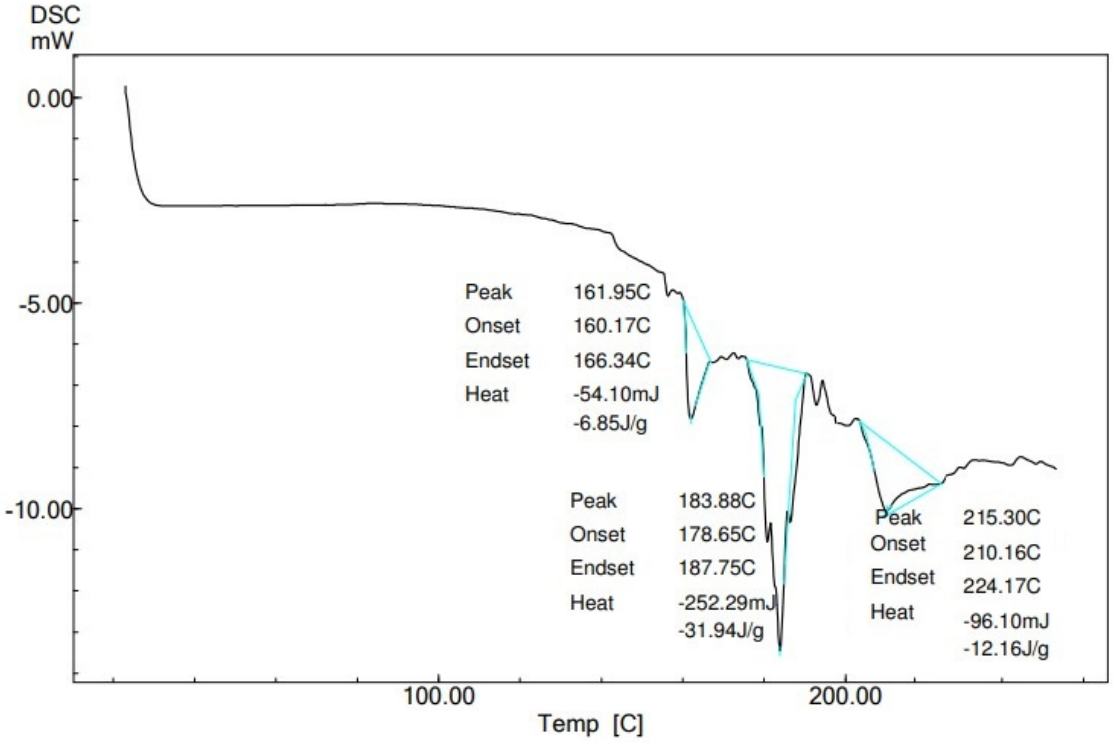

Figure 12: DSC thermal peaks of formulation SD.

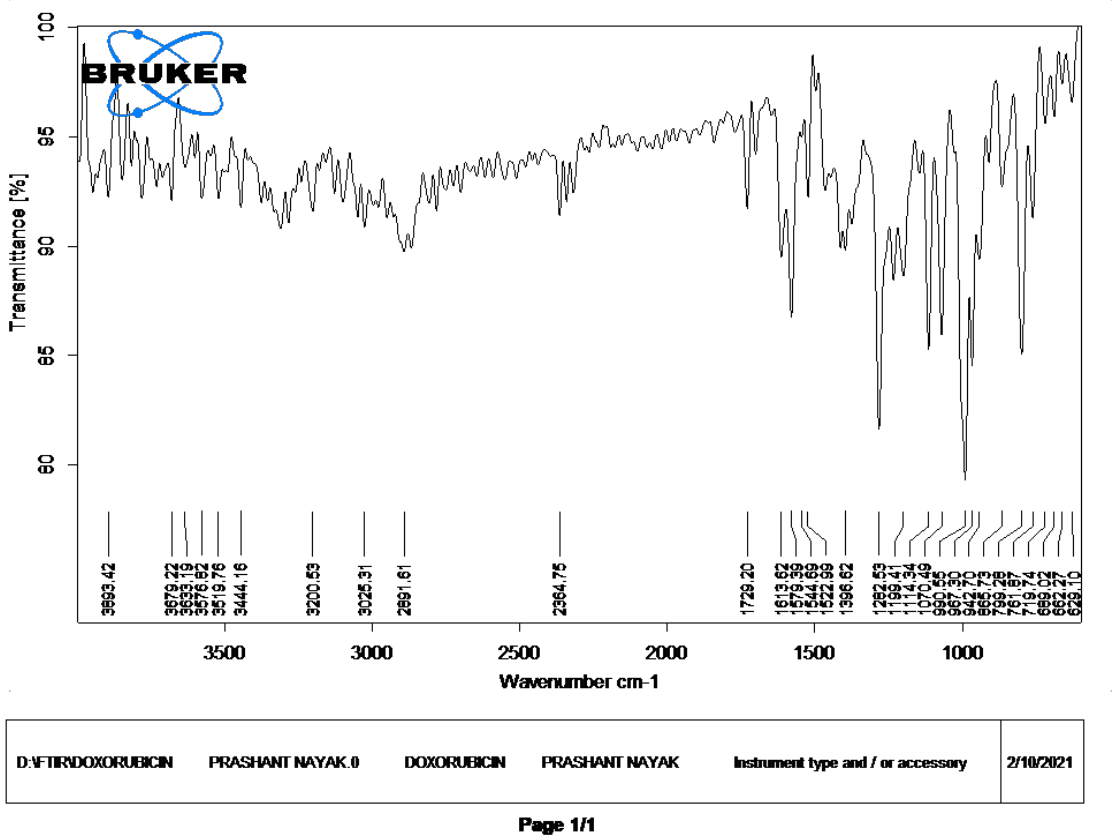

Figure 13: FTIR spectra of doxorubicin.

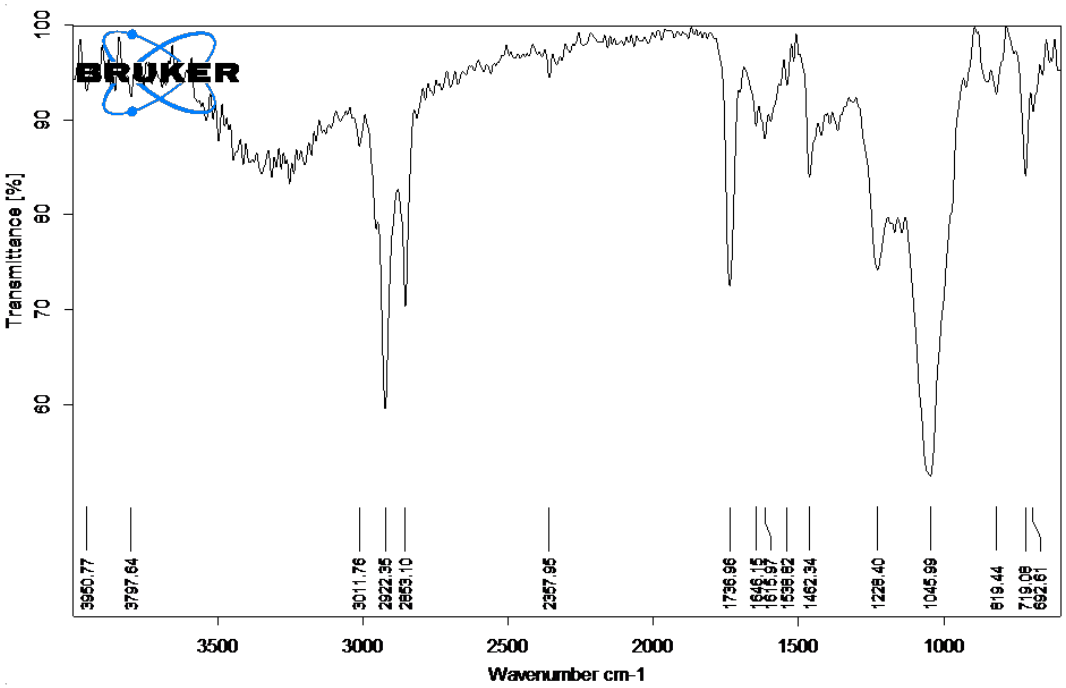

Figure 14: FTIR spectra of Sphingolipid.

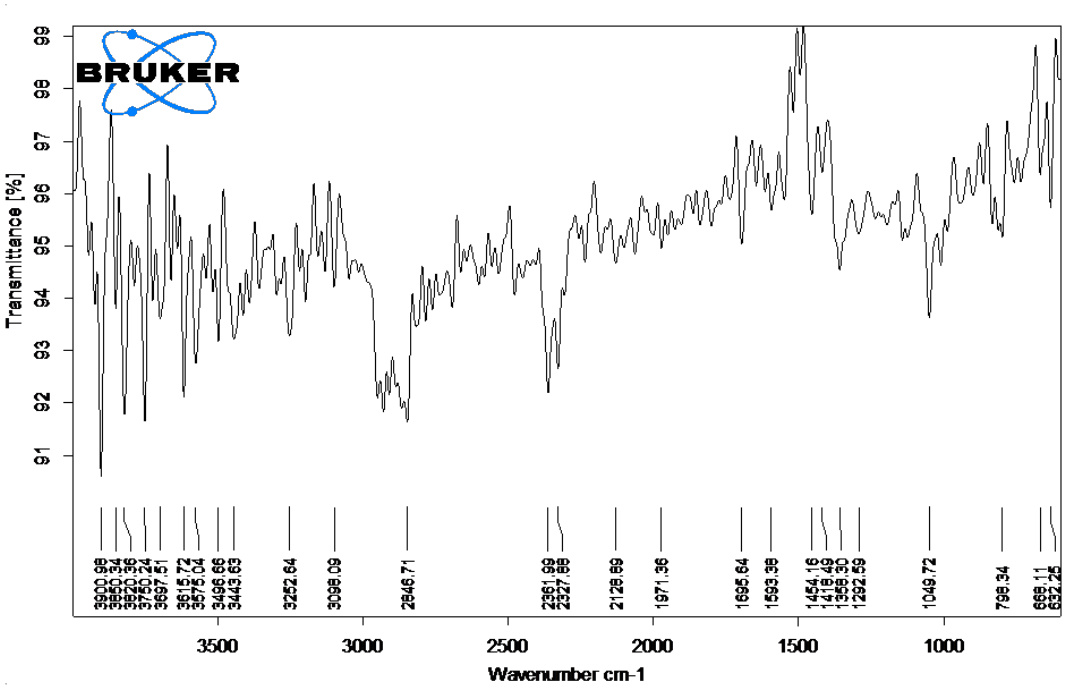

Figure 15: FTIR spectra of cholesterol.

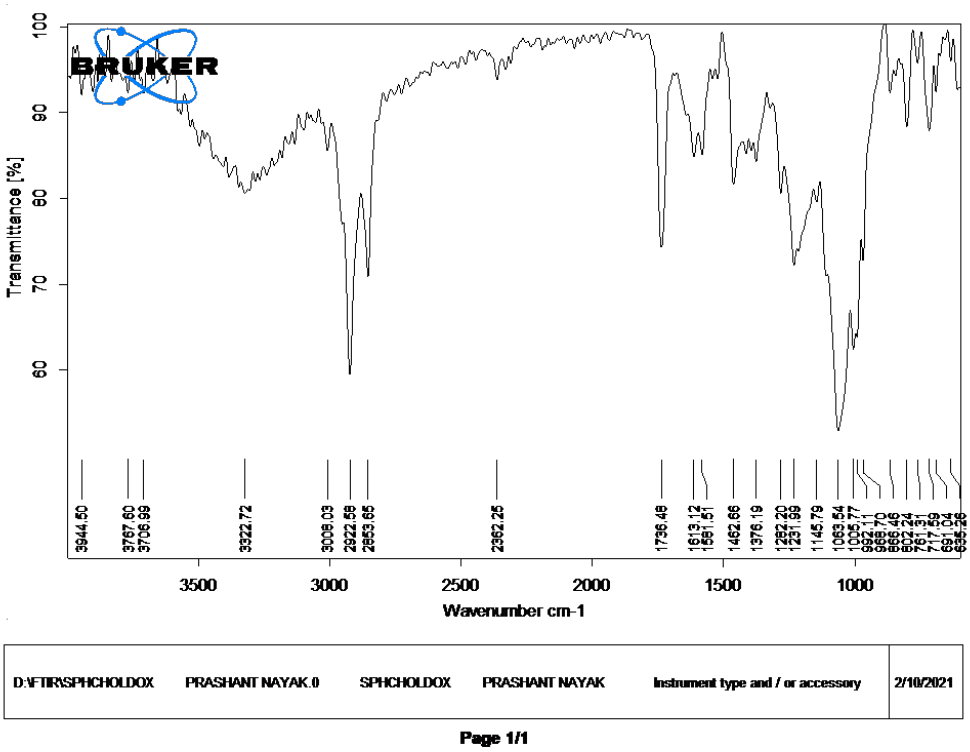

Figure 16: FTIR spectra of physical mixture of doxorubicin, sphingolipids and cholesterol.

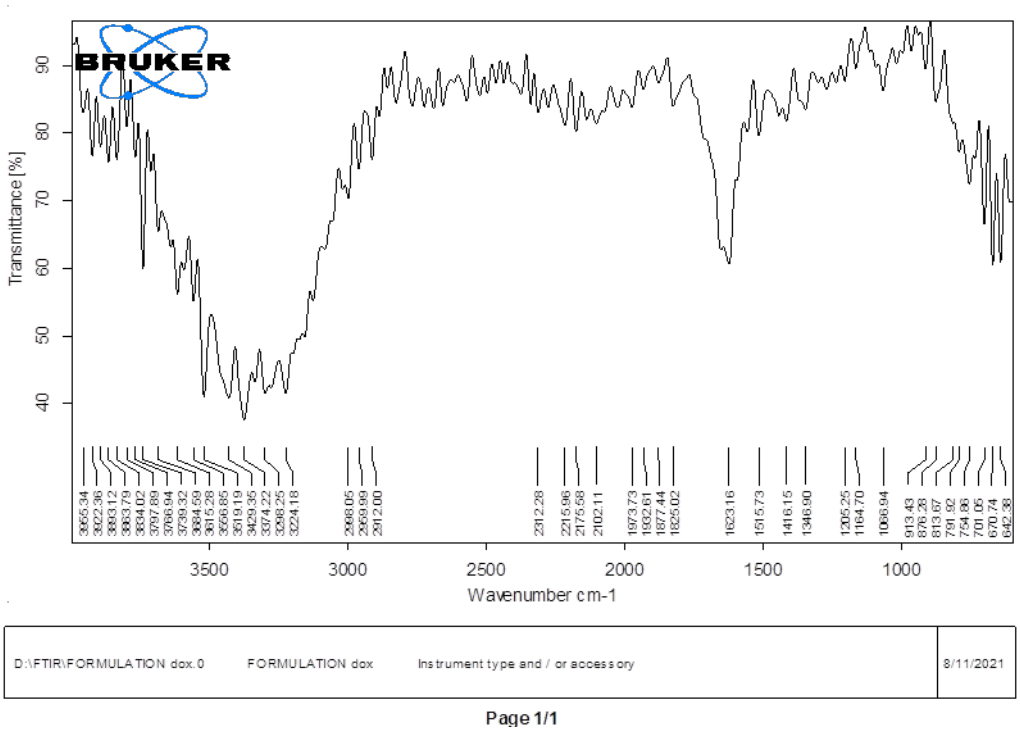

Figure 17: FTIR of optimized formulation transmission vs wavenumber.

the formulation, suggesting slight interaction without significant deviation.

Sphingomyelin: The thermal peak was 178.25°C for the pure drug and 183.88°C in the formulation, indicating the stability of sphingomyelin within the formulation.

These findings, supported by Figures 9-12 and Table 17, confirm that the thermal properties of the formulation components are within their respective ranges. This consistency indicates that there is no significant incompatibility or interaction among the components that would compromise the formulation's stability

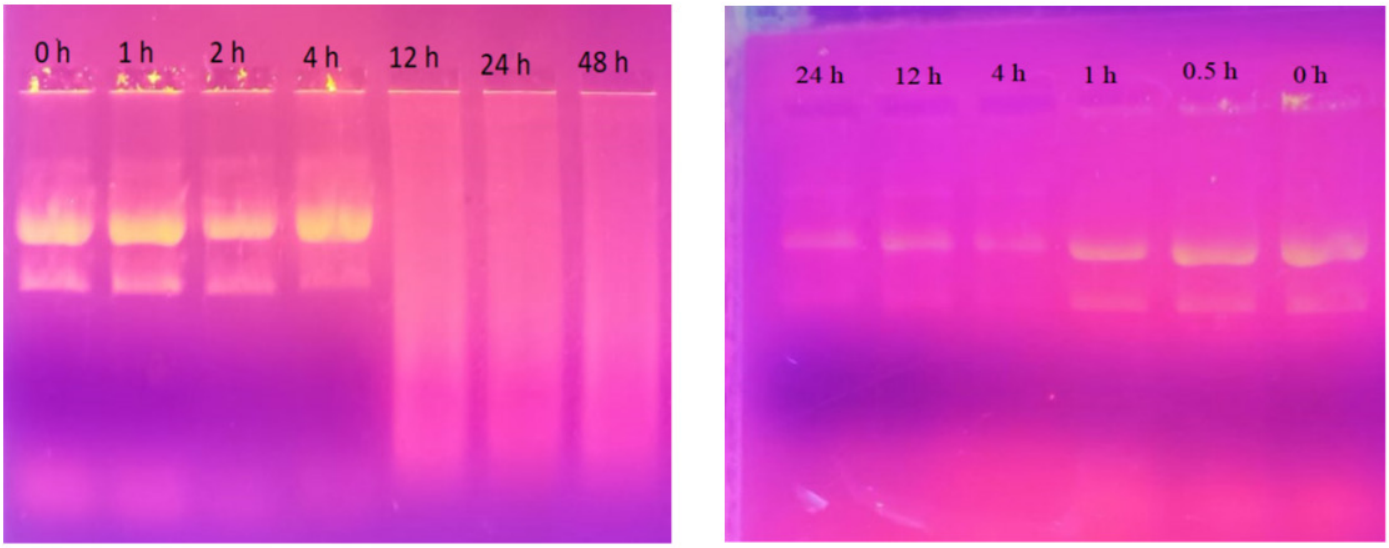

Figure 18: A. Serum stability of siRNA loaded, B. Serum stability of naked si RNA formulation.

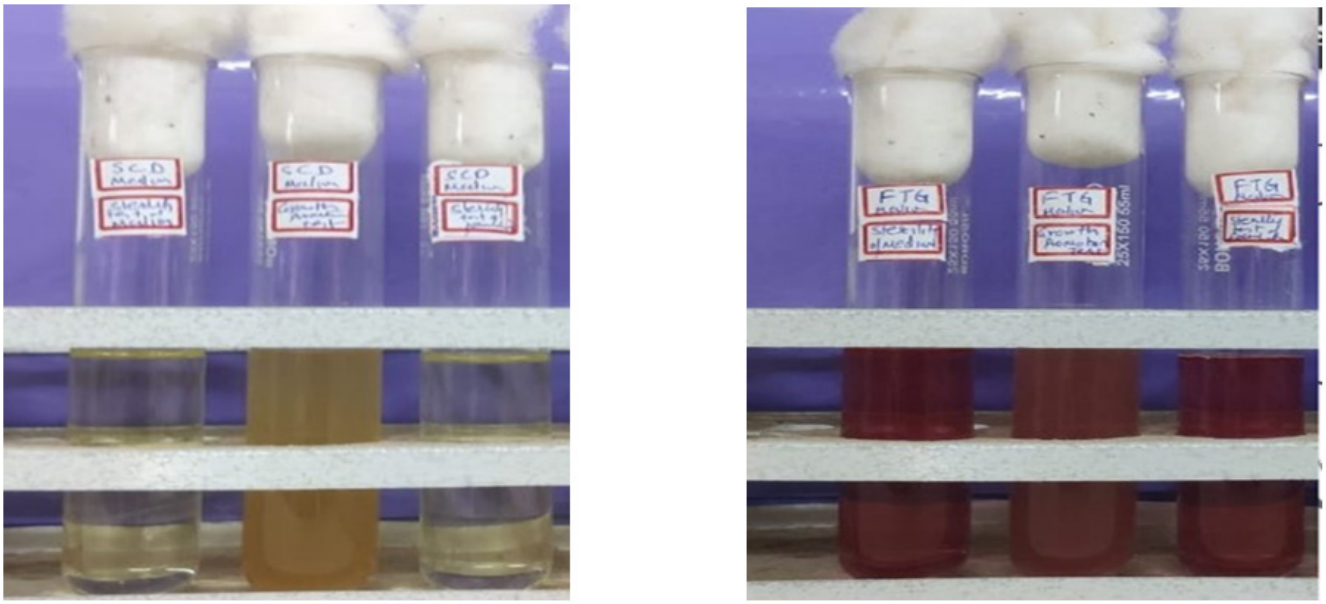

Figure 19: A and B. Sterility test images of optimsed formulation (A) fungus (B) bacteria.

or efficacy. The DSC analysis shows that the formulation's thermal properties are compatible with those of the individual components. This supports the overall stability and integrity of the formulation, ensuring its suitability for therapeutic use.

The FTIR spectra for the pure drug, sphingolipid, cholesterol, physical mixture, and final formulation were analyzed for functional groups, with key peaks listed in the table.

C=O Stretching: Dox showed a peak at 1729 cm^{-1}, sphingolipid and the physical mixture at 1736 cm^{-1}, and the formulation at 1623 cm^{-1}.

O-H Stretching: Peaks were at 3633 cm^{-1} for dox, 3797 cm^{-1} for sphingolipid, 3615 cm^{-1} for cholesterol, 3706 cm^{-1} for the physical mixture, and 3739 cm^{-1} for the formulation.

NH2 Stretching: Dox had a peak at 3519 cm^{-1}, the physical mixture at 3322 cm^{-1}, and the formulation at 3374 cm^{-1}.

-O- Stretching: Peaks were at 1199 cm^{-1} for dox, 1228 cm^{-1} for sphingolipid, 1231 cm^{-1} for the physical mixture, and 1205 cm^{-1} for the formulation.

The comparison showed that the peaks in the physical mixture and formulation were within expected ranges, indicating no significant interactions or incompatibilities among the compounds. The

FTIR analysis confirmed the chemical compatibility and stability of the formulation components, supporting the integrity and consistency of the final product, which is crucial for the efficacy and safety of the sphingosome formulation.

Serum stability studies

The stability of naked siRNA and siRNA in the formulation was assessed through visual analysis of band intensities (Figure 18A and 18B). Naked siRNA was intact for up to 1 hr, partially degraded after 1 hr, and completely degraded by 4 hr. In contrast, siRNA in the formulation remained intact for up to 4 hr, partially degraded at 12 hr, and completely degraded by 48 hr.

These results highlight the formulation's protective effect against nuclease digestion, significantly extending siRNA stability. This extended stability is critical for the therapeutic efficacy and bioavailability of siRNA-based therapies.

Sterility test

The sterility of the formulated Doxorubicin-Bcl2 siRNA-loaded sphingosomes was evaluated using standard protocols. The formulations were incubated for 14 days at 30° to 35°C in fluid thioglycolate medium and at 20° to 25°C in soybean-casein digest medium, targeting a wide range of potential contaminants.The results, shown in Table 19 and Figures 19A and 19B, revealed no microbial growth in any samples, indicating maintained sterility throughout the testing period. This confirms the effectiveness of the production and handling processes in preventing contamination.

Sterility is essential for injectable formulations to prevent infections and ensure the integrity of active components. The sphingosome formulations successfully passed the sterility test, meeting stringent pharmaceutical requirements and supporting their safe clinical use.

CONCLUSION

We have developed a formulation based on 3^2 factorial designs by QBD approach. The software experimental design showed close agreement with experimental value of the optimized formulation thus 3^2 factorial designs was effective for optimizing sphingosomal formulation. The formulation was prepared by thin film hydration method. The particle size of the formulation was found to be 230.7 nm, The PDI of the formulation was found to be 0.195, Result quality of the formulation was found to be good. The zeta potential is -33.4 mV. Entrapment efficiency of the formulation was found to be 75.86%. TEM results proved the particle size was in 200 nm. These thermal peaks were in the respective range on performing the DSC analysis. The thermal peaks of the pure drug and formulation were in the range. In FTIR studies, the physical mixture and the formulation functional group peaks were in the range which confirmed there was no physical incompatibility. Serum stability showed the formulation was stable from nuclease degradation up to 12 hr. A sterility test of 14 days confirmed the formulation was sterile as no growth was observed in the test.

The incorporation of siRNA and Doxorubicin conjugation into the sphingosomal formulation holds significant importance for therapeutic applications. siRNA offers a powerful mechanism for gene silencing, providing a targeted approach to downregulate specific genes involved in disease progression. Conjugating siRNA with Doxorubicin, a well-known chemotherapeutic agent, enhances the therapeutic potential by combining gene therapy with chemotherapy. This dual-action approach not only targets cancer cells more effectively but also minimizes off-target effects, thereby improving the overall treatment efficacy and safety profile.

In conclusion, the optimized sphingosomal formulation exhibits promising characteristics for the delivery of siRNA and Doxorubicin. The successful conjugation of these agents within a stable, biocompatible delivery system underscores the potential of this formulation for advancing cancer therapy, offering a synergistic approach to inhibit tumor growth and proliferation.

ACKNOWLEDGEMENT

This study has been supported by NITTE University and NGSM Institute of Pharmaceutical Sciences Mangalore.

CONFLICT OF INTEREST

The author declares that there is no conflict of interest.

AUTHOR CONTRIBUTION

The authors confirm contribution to the paper as follows: study conception and design: Prashant Nayak, R Narayana Charyulu, A Veena Shetty; data collection: Prashant Nayak; analysis and interpretation of results: R Narayana Charyulu, A Veena Shetty; draft manuscript preparation: Prashant Nayak, R Narayana Charyulu, A Veena Shetty. All authors reviewed the results and approved the final version of the manuscript.

ABBREVIATIONS

NDDS: Nano drug delivery systems; **RNAi:** RNA interference; **DOX:** Doxorubicin; **DoE:** Design of experiments; **RSM:** Response Surface Methodology; **PDI:** Polydispersity index; **TEM:** Transmission electron microscopy; **FTIR:** Fourier Transform Infrared Spectroscopic studies.

REFERENCES

1. Quan XQ, Kang L, Yin XZ, Jin ZH, Gao ZG. Synthesis of pegylated hyaluronic acid for loading dichloro (1, 2-diaminocyclohexane) platinum (II). Chin Chem Lett. 2015;26(6):695-9. doi: 10.1016/j.cclet.2015.04.024.
2. Gupta P, Garcia E, Sarkar A, Kapoor S, Rafiq K, Chand HS, *et al.* Nanoparticle based treatment for cardiovascular diseases. Cardiovascular and haematological disorders-drug targets (formerly current drug targets-cardiovascular and hematological disorders). 2019;19(1):33-44.
3. Cooke JP, Atkins J. Nanotherapeutic solutions for cardiovascular disease. Methodist deBakey Cardiovasc J. 2016;12(3):132-3. doi: 10.14797/mdcj-12-3-132, PMID 27826365.

4. Zhou X, Hao Y, Yuan L, Pradhan S, Shrestha K, Pradhan O, *et al*. Nano-formulations for transdermal drug delivery: a review. Chin Chem Lett. 2018;29(12):1713-24. doi: 10.1016/j.cclet.2018.10.037.
5. Matoba T, Koga JI, Nakano K, Egashira K, Tsutsui H. Nanoparticle-mediated drug delivery system for atherosclerotic cardiovascular disease. J Cardiol. 2017;70(3):206-11. doi: 10.1016/j.jjcc.2017.03.005, PMID 28416142.
6. Singh S, Malik BK, Sharma DK. Molecular drug targets and structure-based drug design: A holistic approach. Bioinformation. 2006;1(8):314-20. doi: 10.6026/97320630001314, PMID 17597912.
7. Fathima KM; *et al*. Sphingosome vescicular system. Int J Pharm Sci Rev Res. 2016;41(1):208-13.
8. Singh S, Malik BK, Sharma DK. Molecular drug targets and structure-based drug design: A holistic approach. Bioinformation. 2006;1(8):314-20. doi: 10.6026/97320630001314, PMID 17597912.
9. Brunke RA. Sphingosomes: properties and potential (liposomes based on sphingolipid). Drug Cosmet Ind. June 1991.
10. Hanabiosciences; 2006. Business Wire. Available from: http://findarticles.com/p/articles/mi_m0EIN/is_/ai_n26798401.
11. Webb MS, Bally MB, Mayor LD. Inex Pharmaceutical Corporation. Sphingosome for enhanced drug delivery.US Patent 5543152; 1996 June 8.
12. Webb MS, Bally MB, Mayor LD. Inex Pharmaceutical Corporation. Sphingosomes for enhanced drug delivery. World Patent 035094. 1995 December 28.
13. Vyas SP, Khar RK. Targeted and controlled drug delivery. 1st ed. New Delhi: CBS publisher; 2002.
14. Talegaonkar S, Mishra P, Khar R, Biju S. Vesicular system: an overview. Indian J Pharm Sci. 2006;68(2):141-53. doi: 10.4103/0250-474X.25707.
15. Holback H, Yeo Y. Intratumoral drug delivery with nanoparticulate carriers. Pharm Res. 2011;28(8):1819-30. doi: 10.1007/s11095-010-0360-y, PMID 21213021.
16. Dinarvand R, Sepehri N, Manoochehri S, Rouhani H, Atyabi F. Polylactide-co-glycolide nanoparticles for controlled delivery of anticancer agents. Int J Nanomedicine. 2011;6:877-95. doi: 10.2147/IJN.S18905, PMID 21720501.
17. Torchilin V. Tumor delivery of macromolecular drugs based on the EPR effect. Adv Drug Deliv Rev. 2011;63(3):131-5. doi: 10.1016/j.addr.2010.03.011, PMID 20304019.
18. Maeda H, Nakamura H, Fang J. The EPR effect for macromolecular drug delivery to solid tumors: improvement of tumor uptake, lowering of systemic toxicity, and distinct tumor imaging in vivo. Adv Drug Deliv Rev. 2013;65(1):71-9. doi: 10.1016/j.addr.2012.10.002, PMID 23088862.
19. Fire A, Xu S, Montgomery MK, Kostas SA, Driver SE, Mello CC. Potent and specific genetic interference by double-stranded RNA in Caenorhabditis elegans. Nature. 1998;391(6669):806-11. doi: 10.1038/35888, PMID 9486653.
20. Hammond SM, Bernstein E, Beach D, Hannon GJ. An RNA-directed nuclease mediates post-transcriptional gene silencing in Drosophila cells. Nature. 2000;404(6775):293-6. doi: 10.1038/35005107, PMID 10749213.
21. Elbashir SM, Harborth J, Lendeckel W, Yalcin A, Weber K, Tuschl T. Duplexes of 21-nucleotide RNAs mediate RNA interference in cultured mammalian cells. Nature. 2001;411(6836):494-8. doi: 10.1038/35078107, PMID 11373684.
22. Hannon GJ, Rossi JJ. Unlocking the potential of the human genome with RNA interference. Nature. 2004;431(7006):371-8. doi: 10.1038/nature02870, PMID 15372045.
23. Merritt WM, Lin YG, Han LY, Kamat AA, Spannuth WA, Schmandt R, *et al*. Dicer, Drosha, and outcomes in patients with ovarian cancer. N Engl J Med. 2008;359(25):2641-50. doi: 10.1056/NEJMoa0803785, PMID 19092150.
24. Wen G, Partridge MA, Li B, Hong M, Liao W, Cheng SK, *et al*. TGFBI expression reduces in vitro and in vivo metastatic potential of lung and breast tumor cells. Cancer Lett. 2011;308(1):23-32. doi: 10.1016/j.canlet.2011.04.010, PMID 21561707.
25. Cai WK, Hu J, Li T, Meng JR, Ma X, Yin SJ, *et al*. Activation of histamine H4 receptors decreases epithelial-to-mesenchymal transition progress by inhibiting transforming growth factor-β1 signalling pathway in non-small cell lung cancer. Eur J Cancer. 2014;50(6):1195-206. doi: 10.1016/j.ejca.2013.12.025, PMID 24447834.
26. Filyak Y, Filyak O, Souchelnytskyi S, Stoika R. Doxorubicin inhibits TGF-β signaling in human lung carcinoma A549 cells. Eur J Pharmacol. 2008;590(1-3):67-73. doi: 10.1016/j.ejphar.2008.05.030, PMID 18606404.
27. Panis C, Herrera AC, Victorino VJ, Aranome AM, Cecchini R. Screening of circulating TGF-β levels and its clinicopathological significance in human breast cancer. Anticancer Res. 2013;33(2):737-42. PMID 23393376.
28. Tacar O, Sriamornsak P, Dass CR. Doxorubicin: an update on anticancer molecular action, toxicity and novel drug delivery systems. J Pharm Pharmacol. 2013;65(2):157-70. doi: 10.1111/j.2042-7158.2012.01567.x, PMID 23278683.
29. Callaghan R, Luk F, Bebawy M. Inhibition of the multidrug resistance P-glycoprotein: time for a change of strategy? Drug Metab Dispos. 2014;42(4):623-31. doi: 10.1124/dmd.113.056176, PMID 24492893.
30. Yang X, Yi C, Luo N, Gong C. Nanomedicine to overcome cancer multidrug resistance. Curr Drug Metab. 2014;15(6):632-49. doi: 10.2174/1389200215666140926154443, PMID 25255871.
31. Prados J, Melguizo C, Ortiz R, Vélez C, Alvarez PJ, Arias JL, *et al*. Doxorubicin-loaded nanoparticles: new advances in breast cancer therapy. Anticancer Agents Med Chem. 2012;12(9):1058-70. doi: 10.2174/187152012803529646, PMID 22339066.
32. Bagherpour Doun SK, Alavi SE, Koohi Moftakhari Esfahani M, Ebrahimi Shahmabadi H, Alavi F, Hamzei S. Efficacy of cisplatin-loaded poly butyl cyanoacrylate nanoparticles on the ovarian cancer: an in vitro study. Tumour Biol. 2014;35(8):7491-7. doi: 10.1007/s13277-014-1996-8, PMID 24789433.
33. Tan R, Niu M, Zhao J, Liu Y, Feng N. Preparation of vincristine sulfate-loaded poly (butylcyanoacrylate) nanoparticles modified with pluronic F127 and evaluation of their lymphatic tissue targeting. J Drug Target. 2014;22(6):509-17. doi: 10.3109/1061186X.2014.897708, PMID 24625287.
34. Yordanov G, Skrobanska R, Evangelatov A. Entrapment of epirubicin in poly (butylcyanoacrylate) colloidal nanospheres by nanoprecipitation: formulation development and in vitro studies on cancer cell lines. Colloids Surf B Biointerfaces. 2012;92:98-105. doi: 10.1016/j.colsurfb.2011.11.029, PMID 22154011.
35. Tefas LR, Sylvester B, Tomuta I, Sesarman A, Licarete E, Banciu M, *et al*. Development of antiproliferative long-circulating liposomes co-encapsulating doxorubicin and curcumin, through the use of a quality-by-design approach. Drug Des Dev Ther. 2017;11:1605-21. doi: 10.2147/DDDT.S129008, PMID 28579758.
36. Sathish KM, Nisharani SR. Implementation of experimental design methodology and characterization of zolmitriptan loaded chitosan nanoparticles. Int Curr Pharm J. 2017;6(3):16-22.
37. Chaudhary V, Hussain S, Jain V, Prakash V, Khar R, Sharma S. Formulation and characterization of solid lipid nanoparticles containing artemether and lumefantrine for treatment of P. falciparum. Br J Pharm Res. 2017;16(2):1-12. doi: 10.9734/BJPR/2017/26483.
38. Sercombe L, Veerati T, Moheimani F, Wu SY, Sood AK, Hua S. Advances and challenges of liposome assisted drug delivery. Front Pharmacol. 2015;6:286. doi: 10.3389/fphar.2015.00286, PMID 26648870.
39. Al-Ahmady ZS, Chaloin O, Kostarelos K. Monoclonal antibody-targeted, temperature-sensitive liposomes: in vivo tumor chemotherapeutics in combination with mild hyperthermia. J Control Release Off J Control Release Soc. 2014;28:196-332.
40. Gupta S, Kesarla R, Chotai N, Misra A, Omri A. Systematic approach for the formulation and optimization of solid lipid nanoparticles of efavirenz by high pressure homogenization using design of experiments for brain targeting and enhanced bioavailability. BioMed Res Int. 2017;2017:5984014. doi: 10.1155/2017/5984014, PMID 28243600.
41. Yasir M, Sara UV. Solid lipid nanoparticles for nose to brain delivery of haloperidol: in vitro drug release and pharmacokinetics evaluation. Acta Pharm Sin B. 2014;4(6):454-63. doi: 10.1016/j.apsb.2014.10.005, PMID 26579417.
42. Anjum DH. Characterization of nanomaterials with transmission electron microscopy. InIOP Conference Series. IOP Conf Ser.: Mater Sci Eng. 2016;146(1):012001. doi: 10.1088/1757-899X/146/1/012001.
43. Wolska E, Sznitowska M, Krzemińska K, Ferreira Monteiro M. Analytical techniques for the assessment of drug-lipid interactions and the active substance distribution in liquid dispersions of Solid Lipid Microparticles (SLM) produced de novo and reconstituted from spray-dried powders. Pharmaceutics. 2020;12(7):664. doi: 10.3390/pharmaceutics12070664, PMID 32679745.
44. Mukherjee B, Patra B, Layek B, Mukherjee A. Sustained release of acyclovir from nano-liposomes and nano-niosomes: an in vitro study. Int J Nanomedicine. 2007;2(2):213-25. PMID 17722549.
45. Katas H, Alpar HO. Development and characterisation of chitosan nanoparticles for siRNA delivery. J Control Release. 2006;115(2):216-25. doi: 10.1016/j.jconrel.2006.07.021, PMID 16959358.
46. Jagani HV, Josyula VR, Hariharapura RC, Palanimuthu VR, Gang SS. Nanoformulation of siRNA silencing Bcl-2 gene and its implication in cancer therapy. Arzneim Forsch. 2011;61(10):577-86. doi: 10.1055/s-0031-1300556, PMID 22164966.
47. Pharmacopoeia of India, Ministry of Health and Family Welfare. Controller Publ, New Delhi, India. 2007;11.

Cite this article: Nayak P, Charyulu RN, Shetty AV. QBD-Based Optimization and Formulation of Doxorubicin Bcl-2 SIRNA-Loaded Sphingosomes. Int. J. Pharm. Investigation. 2025;15(1):138-58.